



Application of GIS and AHP Method in Forest Fire Risk Zone Mapping: a Study of the Parambikulam Tiger Reserve, Kerala, India

S. Nikhil¹ · Jean Homian Danumah² · Sunil Saha³ · Megha K. Prasad⁴ · A. Rajaneesh⁵ · Pratheesh C. Mammen¹ · R. S. Ajin¹ · Sekhar L. Kuriakose¹

Accepted: 21 April 2021 / Published online: 6 May 2021

© The Author(s), under exclusive licence to Springer Nature Switzerland AG 2021

Abstract

Forest fires are one of the most common natural hazards that occur in the Western Ghats region. There are many protected areas in this part of the Western Ghats; therefore, fire can pose a serious threat to habitats and wildlife. In the past, fires have also affected the Parambikulam Tiger Reserve. The objectives of this study are to demarcate the fire risk zones using GIS techniques and to evaluate the influence of each factor on fire initiation. The following factors are selected for the analysis: land cover types, slope angle, aspect, topographic wetness index, distance from the settlement, distance from the road, distance from the tourist spot, and distance from the anti-poaching camp shed. The analytical hierarchy process method is used to determine the weights, and the ArcGIS and ERDAS Imagine software tools are used to create the fire risk zone map. The area of the prepared map is divided into the following five risk zones: very low, low, moderate, high, and very high. The risk zone map has been validated using fire incidence data for the period from 2002 to 2020 collected from the forest fire portal of the Forest Survey of India. It was found that 71% of fire incidences fall in high-risk and very high-risk zones of the prepared map. The validation using the receiver operating characteristic curve analysis, with an area under ROC curve value of 0.795, confirms the prediction accuracy of the risk zone map. The prepared fire risk zone map will help the planners, officials of the forest, and the disaster management departments to take appropriate mitigation measures in order to prevent future fires and thereby protect the valuable forest resources.

Keywords Analytical hierarchy process · Forest fire · GIS · Parambikulam Tiger Reserve · Western Ghats

Introduction

Forest ecosystems are important constituents of terrestrial biodiversity, and hence the effective management of this natural resource is essential (Soman and Anitha 2020). Fires are one

of the most common hazards that occur in forests worldwide. Fires occur due to natural processes, such as lightning, and due to anthropogenic activities (Abdi et al. 2018; Busico et al. 2019; Manna and Bandyopadhyay 2019). The anthropogenic or human-induced fires occur due to accidents, negligence, or arson (Novo et al. 2020). In addition to deaths, forest fires can pose many direct or indirect damages. Fires can significantly affect regional climate, land surface hydrology, biogeochemical processes, wildlife habitats, and the livelihoods of communities (Ambadan et al. 2020). Forest fires can destruct habitats and the biota (Pastro et al. 2011), resulting in post-fire soil erosion (Chen 2006), land degradation (Nadporozhskaya et al. 2018) or desertification (Santín and Doerr 2016), removal of organic matter and deterioration of soil structure and porosity (Certini 2005), emission of greenhouse gases (Sannigrahi et al. 2020), and release of particulate matter, which cause respiratory, cardiovascular, ophthalmic, and psychiatric problems (Finlay et al. 2012); contaminate air by the fire plumes; and contaminate soil and water due to the deposition of particulate and other materials and due to the fire suppression runoff that contains toxic or hazardous materials (Martin

✉ R. S. Ajin
ajinares@ieee.org; ajinares@gmail.com

¹ Kerala State Emergency Operations Centre (KSEOC), Kerala State Disaster Management Authority (KSDMA), Thiruvananthapuram, Kerala, India

² Centre Universitaire de Recherche et d'Application en Télédétection (CURAT), Université Félix Houphouët-Boigny, Abidjan, Côte d'Ivoire

³ Department of Geography, University of Gour Banga, Malda, West Bengal, India

⁴ Department of Remote Sensing, Bharathidasan University, Tiruchirappalli, Tamil Nadu, India

⁵ Department of Geology, University of Kerala, Thiruvananthapuram, Kerala, India

et al. 2016). The protected areas in the Western Ghats region of Kerala, a biodiversity hotspot, were frequently affected by fires (Ajin et al. 2014, 2016a, 2016b, 2017a, 2017b; Vinod et al. 2016). The Western Ghats is one of the 25 biodiversity hotspots of the world and is home to endemic flora and fauna (Nameer et al. 2001). Hence, it is critically important to demarcate the fire risk zones so that proper mitigation measures can be adopted in order to prevent or minimize the impacts of fire.

Several studies used GIS techniques in order to delineate forest fire risk zones (Ajin et al. 2016c, 2018; Dong et al. 2005; Veena et al. 2017; Yin et al. 2004). Researchers effectively used methods such as fuzzy logic (Gheshlaghi et al. 2020; Soto 2012), frequency ratio (Pradhan et al. 2007), artificial neural network (Dimuccio et al. 2011; Satir et al. 2016), analytical network process (Gheshlaghi 2019; Gheshlaghi et al. 2020), weights of evidence (Ye et al. 2017), logistic regression (Deng et al. 2013; Mohammadi et al. 2014; Pan et al. 2016), support vector machine (Gigović et al. 2019; Hong et al. 2018), random forest (Arpaci et al. 2014; Gigović et al. 2019; Leuenberger et al. 2018; Pourtaghi et al. 2016), and neuro-fuzzy system (Bui et al. 2017; Kaur and Sood 2019) for delineating the fire risk/susceptible zones. Many researchers (Arca et al. 2020; Busico et al. 2019; Eskandari 2017; Eskandari and Miesel 2017; Güngöroğlu 2017; Kayet et al. 2020; Nuthammachot and Stratoulas 2019; Novo et al. 2020; Tiwari et al. 2020) effectively used analytical hierarchy process (AHP) or/and fuzzy-AHP methods for delineating the forest fire susceptible/risk zones.

The Parambikulam Tiger Reserve located in the southern Western Ghats region of India is selected as the study area. The objectives of the study are to delineate the forest fire risk zones in the study area using the AHP method and GIS techniques, to assess the influence of each factor on fire initiation, and to find the reasons for fire occurrence in the study area. Factors such as land cover types, slope angle, aspect, topographic wetness index (TWI), distance from the settlement, distance from the road, distance from the tourist spot, and distance from the anti-poaching camp shed are selected for the forest fire risk zonation.

Study Area

The Parambikulam Tiger Reserve (PKMTR) is situated between $76^{\circ} 30' 0''$ and $76^{\circ} 55' 0''$ E longitudes and $10^{\circ} 15' 0''$ and $10^{\circ} 35' 0''$ N latitudes (Fig. 1). This tiger reserve with a total area of 643.66 km^2 comprises the core area of 390.89 km^2 and the buffer area of 252.77 km^2 (Sreehari and Nameer 2016). The major vegetation types of PKMTR are west coast tropical evergreen forests, west coast tropical semi evergreen forests, southern moist mixed deciduous forests, southern dry mixed deciduous forests, and teak plantation. The major peaks in PKMTR are Karimalagapuram (1438 m), Pandaravarai

(1290 m), Vengoli (1120 m), and Puliyarapadam (1010 m) (Sreehari and Nameer 2016). It has three man-made reservoirs, namely Parambikulam, Thunacadavu, and Peruvuripallam, with a cumulative water spread area of 20.66 km^2 (Jobin and Nameer 2012). The sociocultural relevance of the area is signified by the existence of four indigenous communities, namely Kadar, Muthuvar, Malasar, and Malamalar, which are distributed in the following six tribal colonies: Sungam, Kadas, Kuriarkutty, Pooppara, Fifth colony, and Earth Dam colony (Soman and Anitha 2020). Apart from tiger, PKMTR hosts a wide range of vertebrate and invertebrate wildlife, such as elephant (*Elephas maximus*), gaur (*Bos gaurus*), leopard (*Panthera pardus*), sloth bear (*Melursus ursinus*), spotted deer (*Axis axis*), and sambar deer (*Rusa unicolor*), which are some of the major mammalian fauna.

Materials and Methods

PKMTR falls in the Survey of India (SoI) topographic maps numbered 58 B/10, 58 B/11, 58 B/14, and 58 B/15 at the 1:50,000 scale. The data used in this study include Landsat 8 Operational Land Imager (OLI) satellite images, Shuttle Radar Topography Mission (SRTM) digital elevation model (DEM), SoI topographic maps, Google Earth Pro data, and secondary data collected from the Kerala Forests & Wildlife Department. The thematic layers of factors such as land cover types, slope angle, aspect, TWI, distance from the settlement, distance from the road, distance from the tourist spots, and distance from the anti-poaching camp shed were prepared using ArcGIS 10.6 and ERDAS Imagine 8.4 software tools. The thematic layers of factors such as slope angle, aspect, TWI, distance from the settlement, distance from the road, distance from the tourist spot, and distance from the anti-poaching camp shed were classified using the natural breaks (Jenks) classification method. All the spatial data were projected to Universal Transverse Mercator (WGS 84; 43N). The thematic layers were then resampled with a spatial resolution of 30 m and combined using the Raster calculator tool in the ArcGIS software after assigning the weights determined by the AHP method to generate the forest fire risk zone map. The Microsoft Excel was used to derive the AHP weights. The prepared fire risk zone map was then validated using the fire incidence points for the period from 1 November 2002 to 7 November 2020 collected from the forest fire portal of the Forest Survey of India (FSI). The RStudio software was used for the ROC curve analysis and the area under a receiver operating characteristic curve (AUC) value estimation. The major analysis involved in the mapping process is shown in the flowchart (Fig. 2).

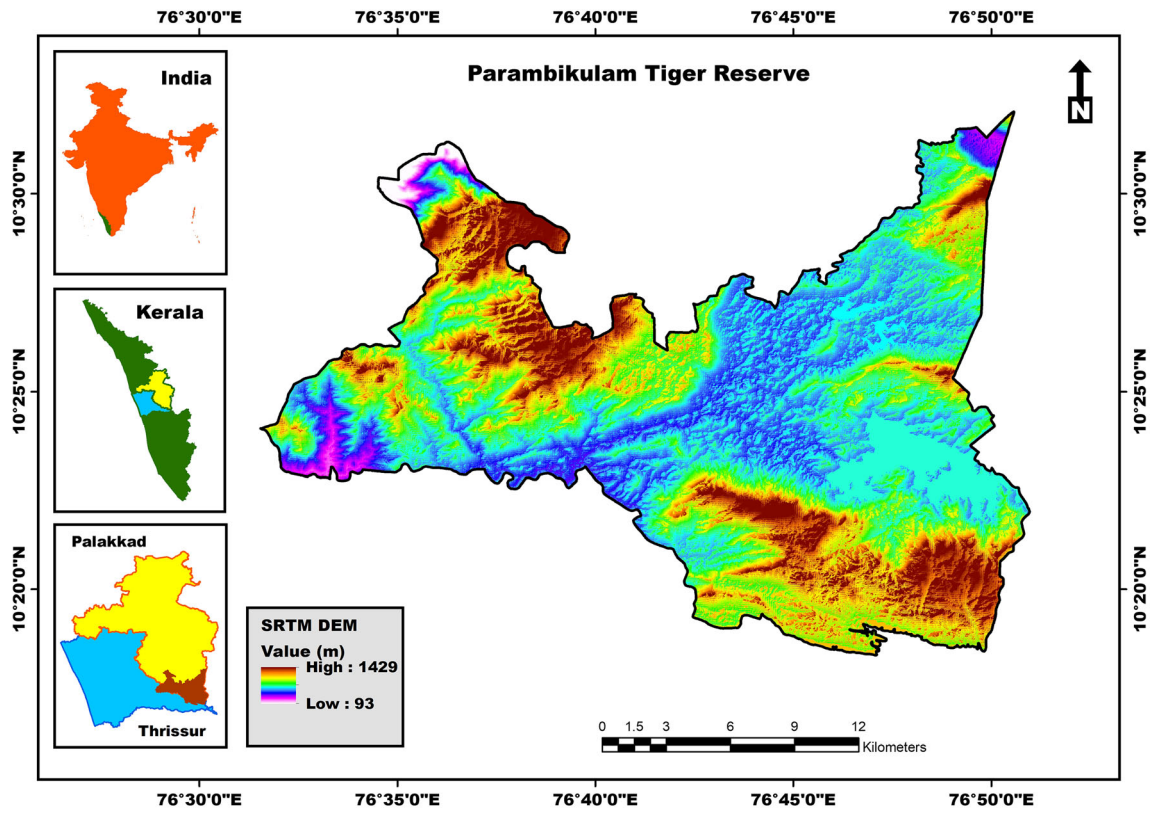


Fig. 1 Study area: Parambikulam Tiger Reserve

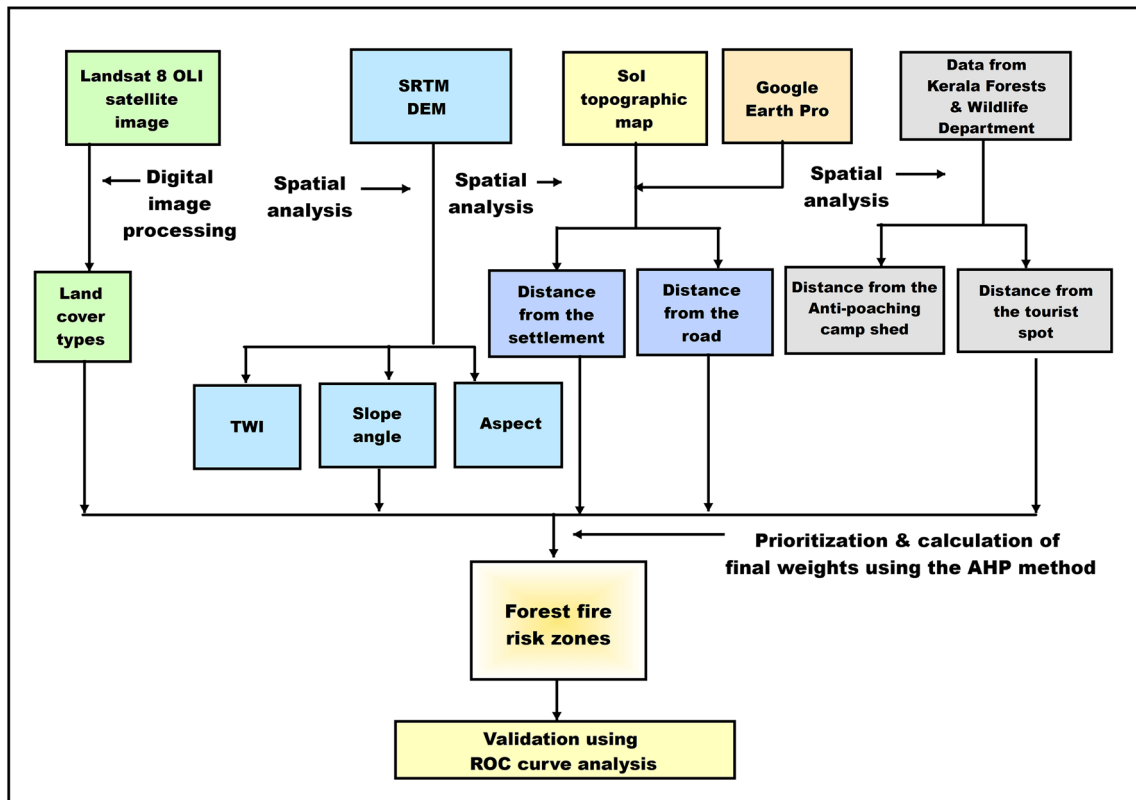


Fig. 2 Flowchart of the method

Causative Factors

Land Cover Types

The vegetation is fuel for the fire, and the fire spread depends on the type of vegetation cover, the fuel spacing, etc. Forest fire is more prevalent in areas where the vegetation is dry and thick (Veena et al. 2017) because flames spread quickly if fuels are closer. The Landsat 8 OLI satellite image with a spatial resolution of 30 m was used to derive the land cover types in the study area. For the supervised classification of the satellite image, the ERDAS Imagine software was used. For classifying different land cover types present in this area, the maximum likelihood (ML) classification method was used. The seven land cover types present in this area are agricultural land, barren land, built-up area, evergreen forest, scrubland, deciduous forest, and water body (Fig. 3).

Slope Angle

The slope is a crucial factor that influences the strength of fire. The steeper slope leads to more fuel preheating (Estes et al. 2017). The spread of fire is faster in uphill areas but slower in downhill areas (Jaiswal et al. 2002). The slope was derived from the SRTM DEM with a spatial resolution of 30 m using the ArcGIS Spatial Analyst (surface analysis) tool. The slope

of the study area is grouped into five classes ($0-7.09^\circ$, $7.09-14.49^\circ$, $14.49-22.50^\circ$, $22.50-32.68^\circ$, and $32.68-78.62^\circ$) as shown in Fig. 4.

Aspect

The aspect of an area influences the fire behavior directly by the amount of solar radiation and moisture availability and indirectly by changes in the vegetation composition and density (Estes et al. 2017). The southern aspects are subjected to greater solar radiation, and the western aspects receive a higher rate of heating (Setiawan et al. 2004). Hence, the southern and western aspects are more prone to fires. The aspect was derived from the SRTM DEM using the ArcGIS Spatial Analyst (surface analysis) tool. The aspect (Fig. 5) is grouped into the following nine classes: Flat, North, Northeast, East, Southeast, South, Southwest, West, and Northwest.

Topographic Wetness Index

TWI refers to the spatial distribution of soil moisture and surface saturation (Yong et al. 2012). Large forest fires exclusively occur under low soil moisture conditions (Krueger et al. 2015). The topographic wetness index was derived from the SRTM DEM with a spatial

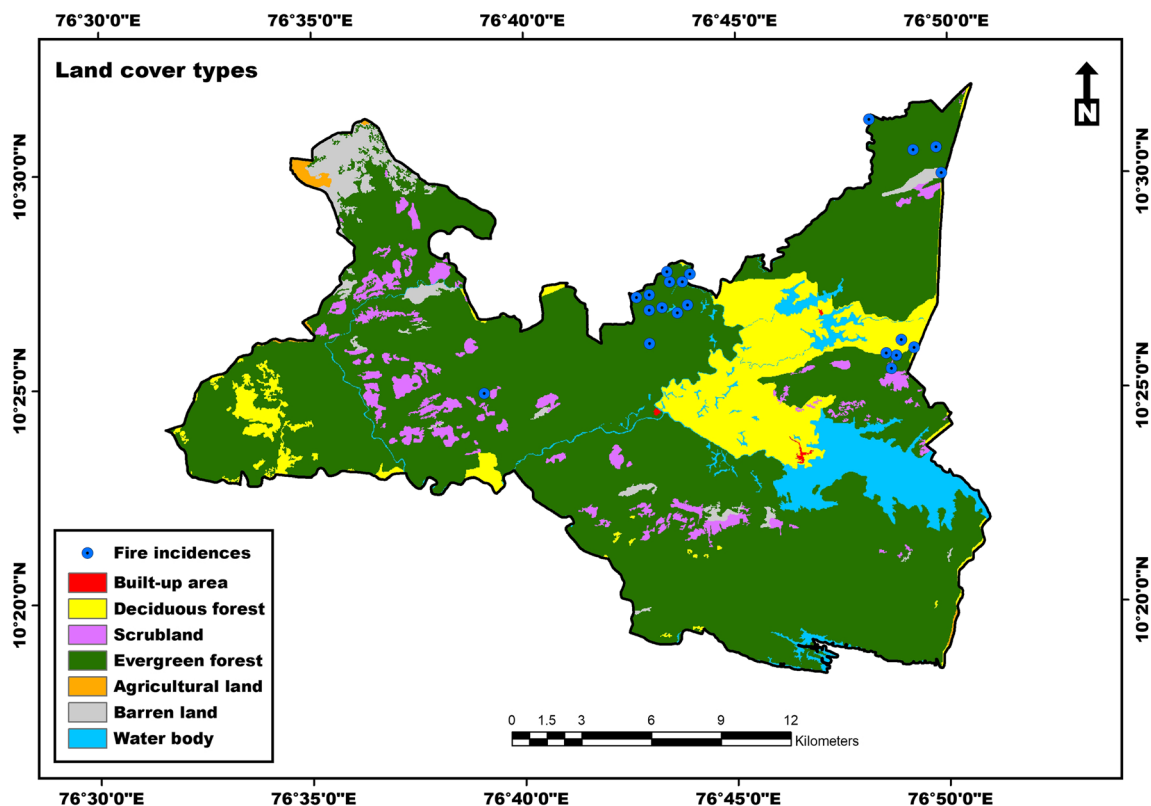


Fig. 3 Land cover types

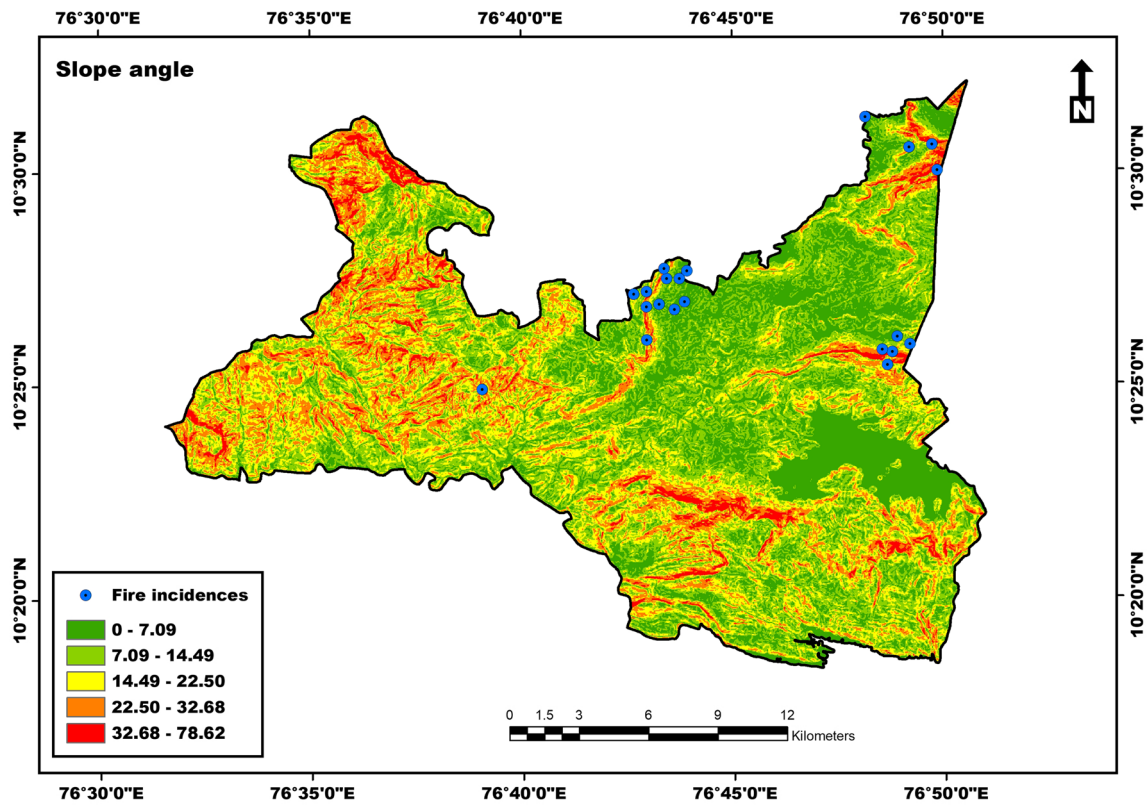


Fig. 4 Slope angle

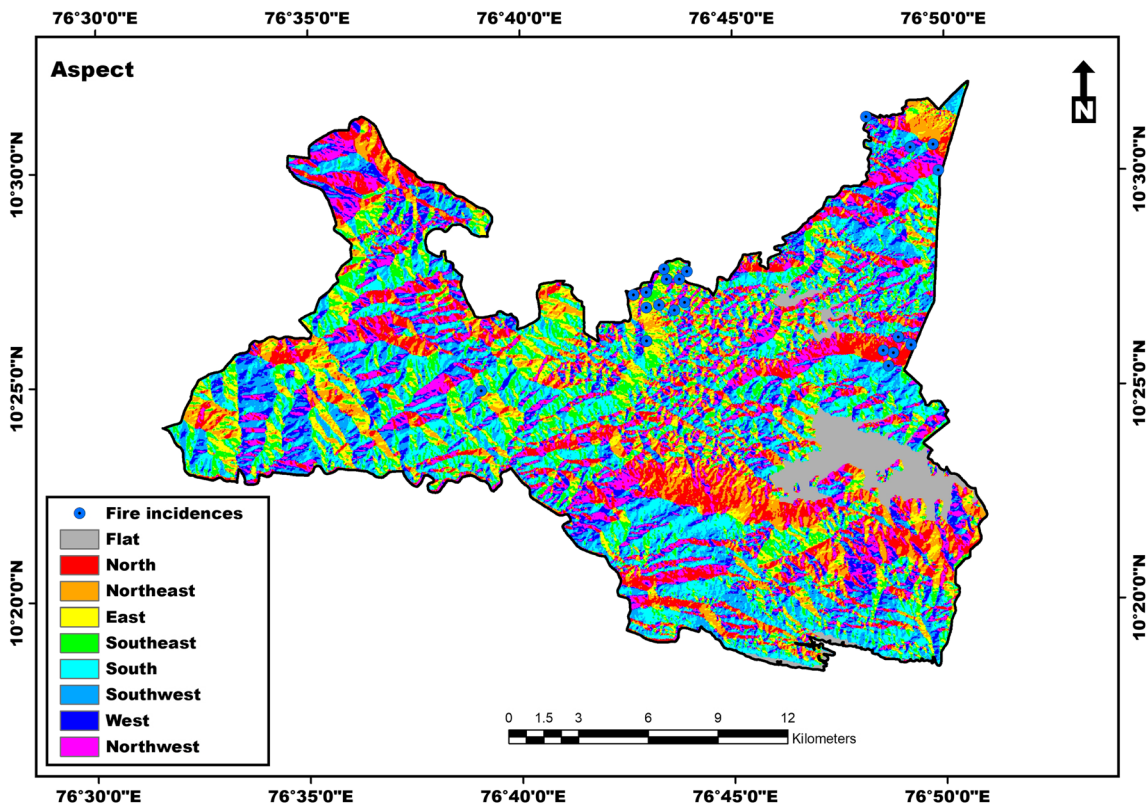


Fig. 5 Aspect

resolution of 30 m. TWI was calculated using Eq. 1 (Beven and Kirkby 1979) and ArcGIS Spatial Analyst tools.

$$\text{TWI} = \ln(\alpha/\tan\beta) \quad (1)$$

where α is the specific catchment area ($A = A/L$, catchment area (A) divided by the contour length (L)) and β is the local slope.

The present study has classified the study area into five classes (1.85–5.41, 5.41–6.81, 6.81–8.83, 8.83–11.70, and 11.70–19.66) based on the topographic wetness index as shown in Fig. 6.

Distance from the Settlement

The expansion of the wildland–urban interface (WUI) can increase the damages, and more people can be at risk (Tedim et al. 2014). Human-induced fires can be intentional or unintentional. The tribes may set fire to scare wild animals away, to make charcoal, and to collect non-timber forest products. When the fire is not fully extinguished, it may escalate to a disastrous forest fire. Unextinguished cigarette butts thrown by people and campfires set by people can also result in the accidental forest fire. Firewood is used by the tribes residing in the surrounding areas for cooking and other purposes. Sparks produced by such burning can eventually lead to a fire in the

nearby forest. Controlled burning is carried out by the forest department in order to avoid large forest fires by burning all the fuel content in the forest before the dry season. Sometimes this fire spreads due to carelessness and leads to large fires. The deliberate forest fires mainly result from the fire set by tribes as a part of tribal traditions, and to clear off the path from dry litter. In some cases, some miscreants also burn forests to settle scores with the forest department and to encroach the forest land. The settlements were digitized from the SoI topographic maps and updated using Google Earth Pro data, and the distance from the settlement layer was generated using the ArcGIS Spatial Analyst (Euclidean distance) tool. PKMTR is divided into five zones (0–2.42 km, 2.42–4.77 km, 4.77–8.05 km, 8.05–11.78 km, and 11.78–16.69 km) based on the distance from the settlements as shown in Fig. 7.

Distance from the Road

The presence of the road is an important factor in the occurrence of human-induced fires (Ricotta et al. 2018). Fires may occur deliberately or accidentally by moving travelers and vehicles on the road (Veena et al. 2017). Wildfire can occur from sparks by cooking near forest roads, campfires set by visitors near forest roads, and coal tar heating for road construction (Satendra and Kaushik 2014) or from refurbishing and repairing existing roads. The roads were digitized from the SoI topographic maps and updated using Google Earth Pro data, and the distance from the

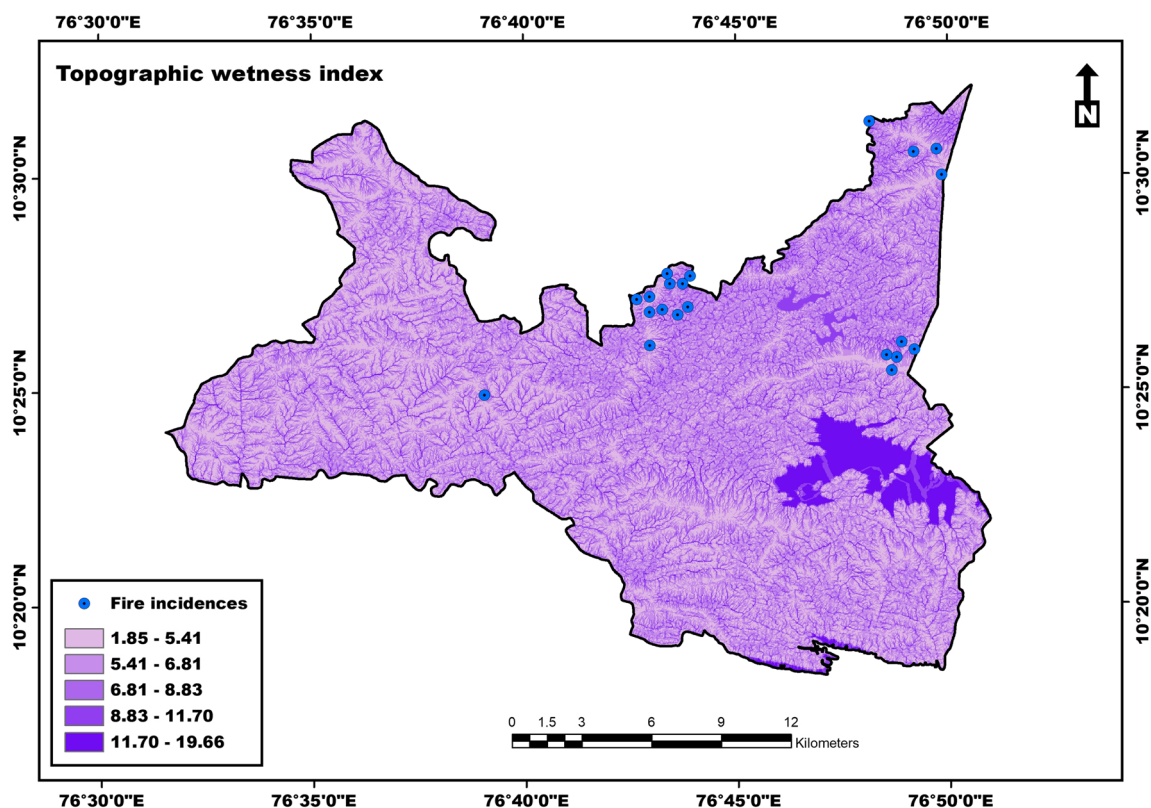


Fig. 6 Topographic wetness index

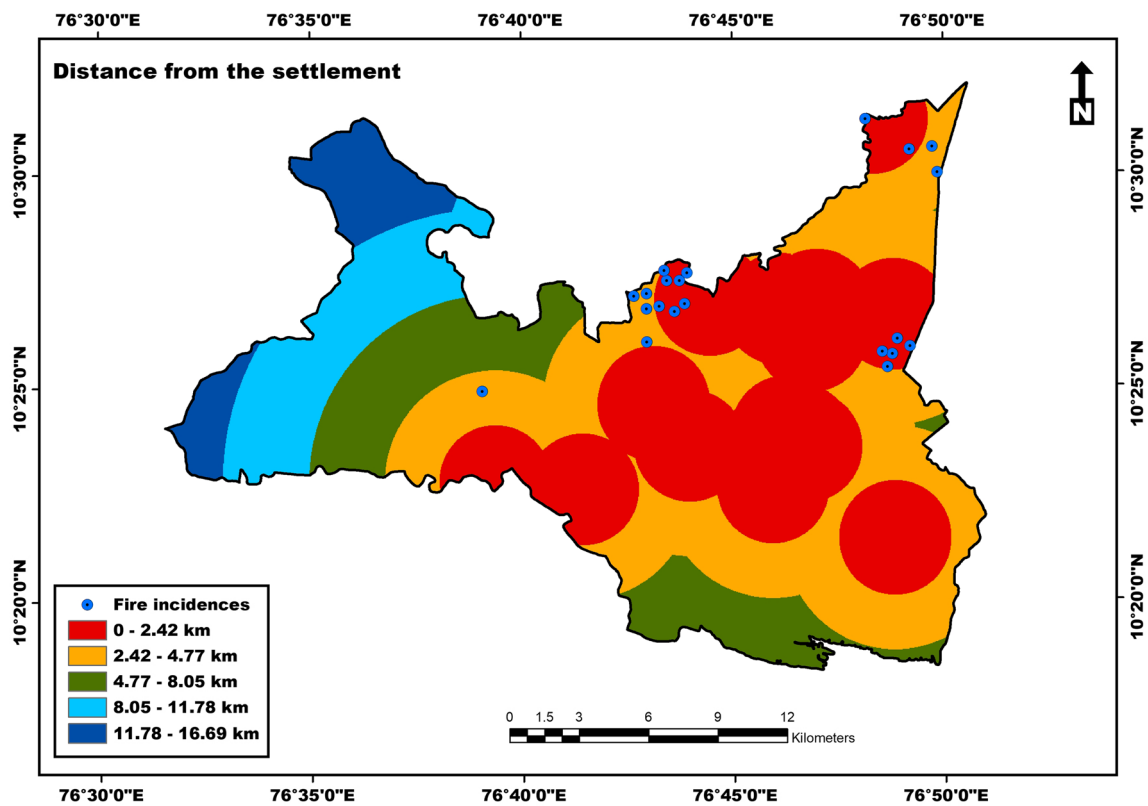


Fig. 7 Distance from the settlement

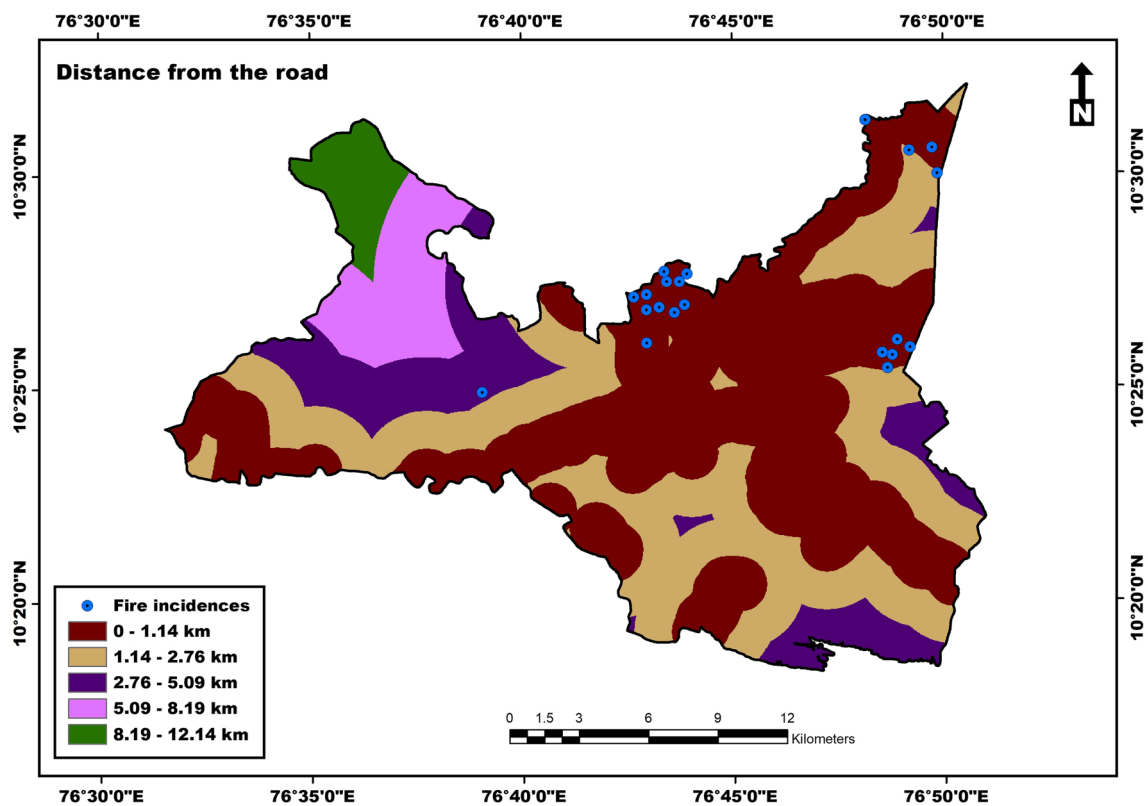


Fig. 8 Distance from the road

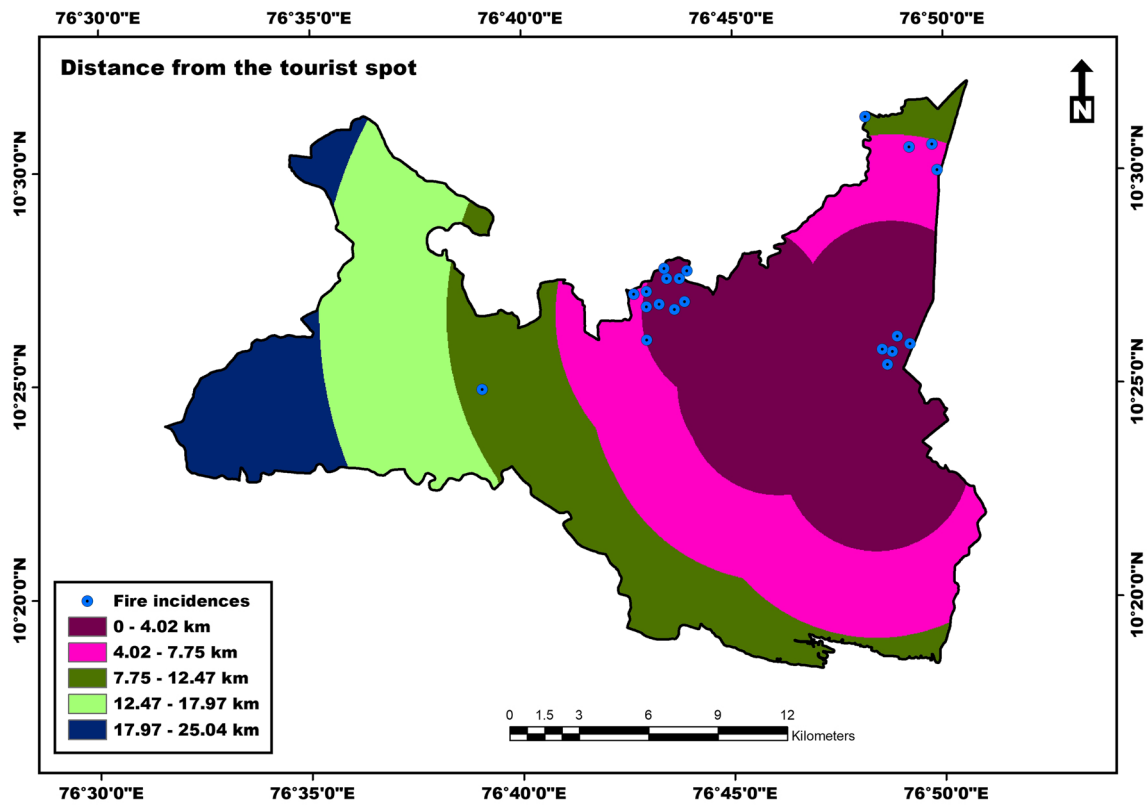


Fig. 9 Distance from the tourist spot

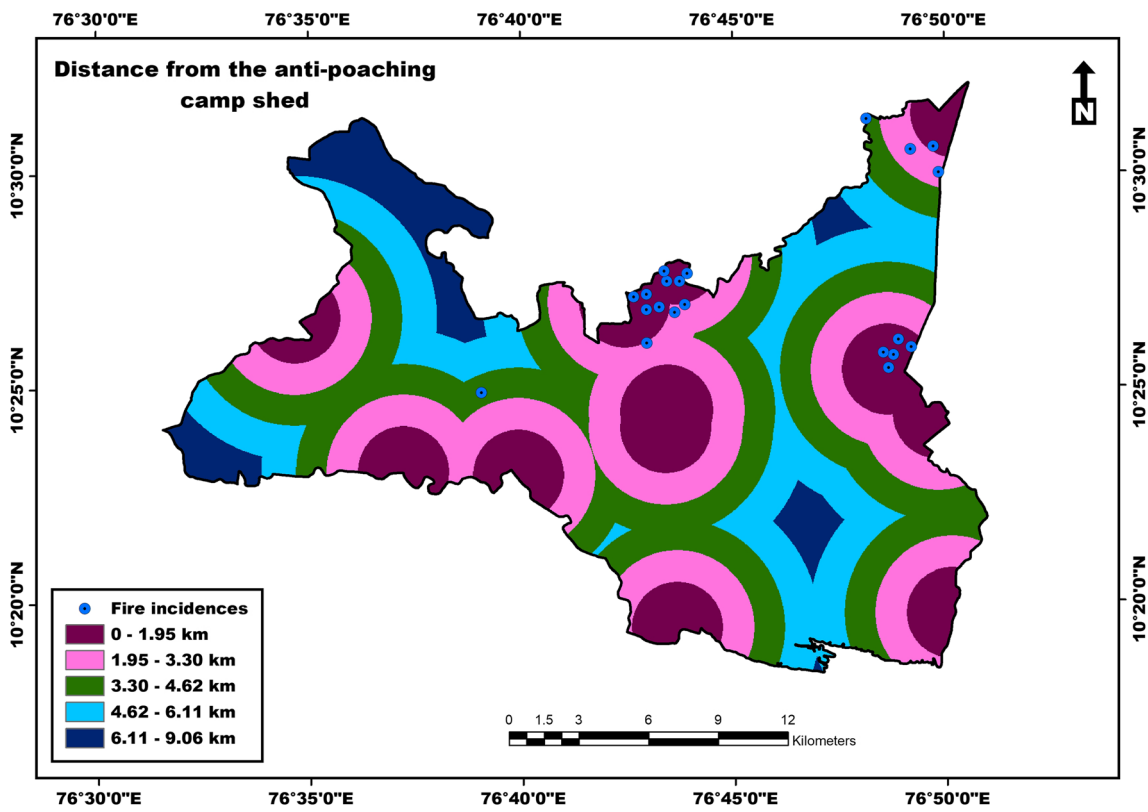


Fig. 10 Distance from the anti-poaching camp shed

Table 1 The Saaty rating scale (Saaty 1980)

| Intensity of scale | Definition | Explanation |
|--------------------|---------------------------|--|
| 1 | Equal importance | 2 factors contribute equally to the objective |
| 3 | Somewhat more important | Experience and judgment slightly favor 1 over the other |
| 5 | Much more important | Experience and judgment strongly favor 1 over the other |
| 7 | Very much more important | Experience and judgment very strongly favor 1 over the other |
| 9 | Absolutely more important | The evidence favoring 1 over the other is of the highest possible validity |
| 2, 4, 6, 8 | Intermediate values | When compromise is needed |

road layer was derived using the spatial analyst (Euclidean distance) tool in the ArcGIS software. Based on the distance from the settlements, PKMTR is classified into five zones (0–1.14 km, 1.14–2.76 km, 2.76–5.09 km, 5.09–8.19 km, and 8.19–12.14 km) as shown in Fig. 8.

Distance from the Tourist Spot

Wildlife sanctuaries, national parks, and tiger reserves provide an ideal environment for recreational activities. The tourists visiting these protected areas can trigger accidental forest fires. The campfires set by tourists, thrown unextinguished cigarettes, and the sparks while they cook near forests may spread fire sometimes and lead to large fires. The location of tourist spots was collected from the Kerala Forest and Wildlife Department. In areas close to tourist spots, the possibility of forest fires is considered high. The spatial analyst (Euclidean distance) tool was used to generate the distance from the tourist spot layer. Based on the distance from the tourist spot, the study area is divided into five zones (0–4.02 km, 4.02–7.75 km, 7.75–12.47 km, 12.47–17.97 km, and 17.97–25.04 km) as shown in Fig. 9.

Table 2 Pairwise comparison matrix

| | LCT | Slp. | Asp. | TWI | DS | DR | DTS | DAPCS |
|-------|------|------|------|-------|-------|-------|-------|-------|
| LCT | 1 | 2 | 3 | 4 | 5 | 6 | 7 | 8 |
| Slp. | 1/2 | 1 | 2 | 3 | 4 | 5 | 6 | 7 |
| Asp. | 1/3 | 1/2 | 1 | 2 | 3 | 4 | 5 | 6 |
| TWI | 1/4 | 1/3 | 1/2 | 1 | 2 | 3 | 4 | 5 |
| DS | 1/5 | 1/4 | 1/3 | 1/2 | 1 | 2 | 3 | 4 |
| DR | 1/6 | 1/5 | 1/4 | 1/3 | 1/2 | 1 | 2 | 3 |
| DTS | 1/7 | 1/6 | 1/5 | 1/4 | 1/3 | 1/2 | 1 | 2 |
| DAPCS | 1/8 | 1/7 | 1/6 | 1/5 | 1/4 | 1/3 | 1/2 | 1 |
| Σ | 2.72 | 4.59 | 7.45 | 11.28 | 16.08 | 21.83 | 28.50 | 36.00 |

LCT land cover types, Slp. slope angle, Asp. aspect, TWI topographic wetness index, DS distance from the settlement, DR distance from the road, DTS distance from the tourist spot, DAPCS distance from the anti-poaching camp shed

Distance from the Anti-poaching Camp Shed

Anti-poaching camp sheds are established across the protected areas in order to effectively manage the largely inaccessible areas. These buildings serve as base camps from which forest managers can perambulate the area that helps monitor the poaching and other illegal activities within the forest. Smugglers and poachers initiate forest fires for concealing the stumps of illegal felling. Anti-poaching camp sheds also act as fire-monitoring stations throughout the fire season. A well-equipped camp shed can respond quickly during an emergency, as time is the limiting factor in certain areas that are difficult to reach. The anti-poaching camp sheds may also impact the forest area if the staff handle fire sources irresponsibly. The areas close to camp sheds are usually less likely affected because they are strictly supervised. The location of anti-poaching camp sheds was collected from the Kerala Forest and Wildlife Department. The spatial analyst (Euclidean distance) tool in the ArcGIS software was used to prepare the distance from the anti-poaching camp shed layer. Based on the distance from the anti-poaching camp shed, the study area is divided into five zones (0–1.95 km, 1.95–3.30 km, 3.30–4.62 km, 4.62–6.11 km, and 6.11–9.06 km) as shown in Fig. 10.

Table 3 Eigenvector and weighting coefficient

| | Vp | Cp |
|-------|-------|------|
| LCT | 3.76 | 0.33 |
| Slp. | 2.66 | 0.23 |
| Asp. | 1.82 | 0.16 |
| TWI | 1.22 | 0.11 |
| DS | 0.82 | 0.07 |
| DR | 0.55 | 0.05 |
| DTS | 0.38 | 0.03 |
| DAPCS | 0.27 | 0.02 |
| Σ | 11.48 | 1.00 |

Table 4 Normalized matrix

| | LCT | Slp. | Asp. | TWI | DS | DR | DTS | DAPCS | Σ of rank | [C] | [D] = [A] × [C] | [E] = [D]/[C] | λ _{max} | CI | CR |
|-------|------|------|------|------|------|------|------|-------|-----------|------|-----------------|---------------|------------------|------|------|
| LCT | 0.37 | 0.44 | 0.40 | 0.35 | 0.31 | 0.27 | 0.25 | 0.22 | 2.61 | 0.33 | 2.78 | 8.51 | 8.29 | 0.04 | 0.03 |
| Slp. | 0.18 | 0.22 | 0.27 | 0.27 | 0.25 | 0.23 | 0.21 | 0.19 | 1.82 | 0.23 | 1.94 | 8.55 | | | |
| Asp. | 0.12 | 0.11 | 0.13 | 0.18 | 0.19 | 0.18 | 0.18 | 0.17 | 1.25 | 0.16 | 1.33 | 8.47 | | | |
| TWI | 0.09 | 0.07 | 0.07 | 0.09 | 0.12 | 0.14 | 0.14 | 0.14 | 0.86 | 0.11 | 0.90 | 8.33 | | | |
| DS | 0.07 | 0.05 | 0.04 | 0.04 | 0.06 | 0.09 | 0.11 | 0.11 | 0.59 | 0.07 | 0.60 | 8.17 | | | |
| DR | 0.06 | 0.04 | 0.03 | 0.03 | 0.03 | 0.05 | 0.07 | 0.08 | 0.40 | 0.05 | 0.40 | 8.07 | | | |
| DTS | 0.05 | 0.04 | 0.03 | 0.02 | 0.02 | 0.02 | 0.04 | 0.06 | 0.27 | 0.03 | 0.27 | 8.07 | | | |
| DAPCS | 0.05 | 0.03 | 0.02 | 0.02 | 0.02 | 0.02 | 0.02 | 0.03 | 0.19 | 0.02 | 0.20 | 8.16 | | | |
| Σ | 1.00 | 1.00 | 1.00 | 1.00 | 1.00 | 1.00 | 1.00 | 1.00 | 8.00 | 1.00 | | 66.33 | | | |

Prioritization and Calculation of Final Weights Using the AHP Method

The AHP method (Saaty 1980) can be used to efficiently evaluate complex decisions. By testing the accuracy of evaluations, the AHP method reduces bias in the decision-making process. For the construction of the judgment matrix, a 1–9 scale (Table 1) is used in the AHP modeling. The major steps involved in the AHP method are constructing a matrix for pair-wise comparisons (Table 2), eigenvector and weighting coefficient calculation (Table 3), and consistency ratio calculation (Table 4).

The eigenvector (Vp) is calculated using Eq. 2 as follows:

$$Vp = \sqrt[k]{W1x...Wk} \tag{2}$$

where *k* is the number of factors, and *W* is the ratings of the factors.

The weighting coefficient (Cp) is calculated using Eq. 3 as follows:

$$Cp = \frac{Vp}{Vp1 + ...Vpk} \tag{3}$$

The sum of Cp of all parameters of a matrix must be equal to 1.

The matrix is normalized by dividing each element by the sum of the column. By averaging each row, the priority vector, [C], is calculated. The overall priority, [D], is calculated by multiplying each column of the matrix by the corresponding priority vector. The rational priority, [E], is determined by dividing each overall priority by the priority vector.

Table 5 Random index (Saaty 1980)

| | Number of criteria | | | | | | | | | |
|----|--------------------|------|------|------|------|------|------|------|------|------|
| | 2 | 3 | 4 | 5 | 6 | 7 | 8 | 9 | 10 | 11 |
| RI | 0.00 | 0.58 | 0.90 | 1.12 | 1.24 | 1.32 | 1.41 | 1.45 | 1.49 | 1.51 |

The eigenvalue (λ_{max}) is determined using Eq. 4 as follows:

$$\lambda_{max} = \frac{[E]}{k} \tag{4}$$

The consistency index (CI) is calculated using Eq. 5 as follows:

$$CI = (\lambda_{max} - k) / (k - 1) \tag{5}$$

The consistency ratio (CR) is determined using Eq. 6 as follows:

$$CR = \frac{CI}{RI} \tag{6}$$

where RI is the random index. RI is the average CI depending on the order *k* of the matrix (Kil et al. 2016) and utilizes the value given by Saaty (1980) as in Table 5.

The CR should be less than 0.1; otherwise, the judgments are not credible, and the exercises should be repeated (Saaty 1980). In this analysis, CR is 0.030 (less than 0.1), so the judgments are reliable.

The final weights obtained using the AHP method is shown in Eq. 7:

$$FRZ = (0.33 \times LCT) + (0.23 \times Slp.) + (0.16 \times Asp.) + (0.11 \times TWI) + (0.07 \times DS) + (0.05 \times DR) + (0.03 \times DTS) + (0.02 \times DAPCS) \tag{7}$$

Validation of the Result

The prepared fire risk zone map was validated using the ROC curve analysis. The ROC analysis investigates the relationship between the sensitivity (true positive rate) and specificity (true negative rate) of a binary classifier (Flach 2011). The ROC curve is the plot of the sensitivity versus 1 – the specificity (Franzen 2011). The AUC is a single scalar value that

Table 6 Area and percentage of risk zones and fire incidence details

| Forest fire risk zones | Area (km ²) | Percentage of the area of the fire risk zones | No. of fire incidences | Percentage of fire incidences |
|------------------------|-------------------------|---|------------------------|-------------------------------|
| Very low | 30.57 | 4.75 | 0 | 0.00 |
| Low | 39.26 | 6.10 | 0 | 0.00 |
| Moderate | 175.27 | 27.23 | 6 | 28.57 |
| High | 249.80 | 38.81 | 9 | 42.86 |
| Very high | 148.76 | 23.11 | 6 | 28.57 |
| Total | 643.66 | 100 | 21 | 100 |

measures the overall performance of a binary classifier (Hanley and McNeil 1982). The AUC value ranges between 0.5 and 1, where the minimum value represents the performance of a random classifier, and the maximum value indicates a perfect classifier (Melo 2013). The AUC result was outstanding for values above 0.9, excellent for values between 0.8 and 0.9, and acceptable for values between 0.7 and 0.8 (Hosmer and Lemeshow 2000).

Results and Discussion

Forest fire risk zones in PKMTR were demarcated using the AHP method and geospatial tools (Fig. 11). The area of the forest fire risk map was divided into the following five risk

zones: very low, low, moderate, high, and very high (Table 6). A total of 21 fire incidents were recorded in PKMTR during the period from November 2002 to November 2020. By overlaying the incidence points over the risk zone map, it was found that 15 (71%) fire incidences spatially fall over the high-risk and very high-risk zones. In this area, the angle of slope and the land cover types do not show a significant influence on fire occurrence. Most of the fires occurred in areas that are covered with evergreen forest than the deciduous forest, and only five fires were recorded on higher slopes. The surface moisture plays an important role in fire occurrence. The majority of the fires occurred in areas with lesser moisture content. It was found that most of the fire incidences occurred in the vicinity of settlements (14 fire incidences) and roads (18 fire incidences). This confirms the anthropogenic origin of

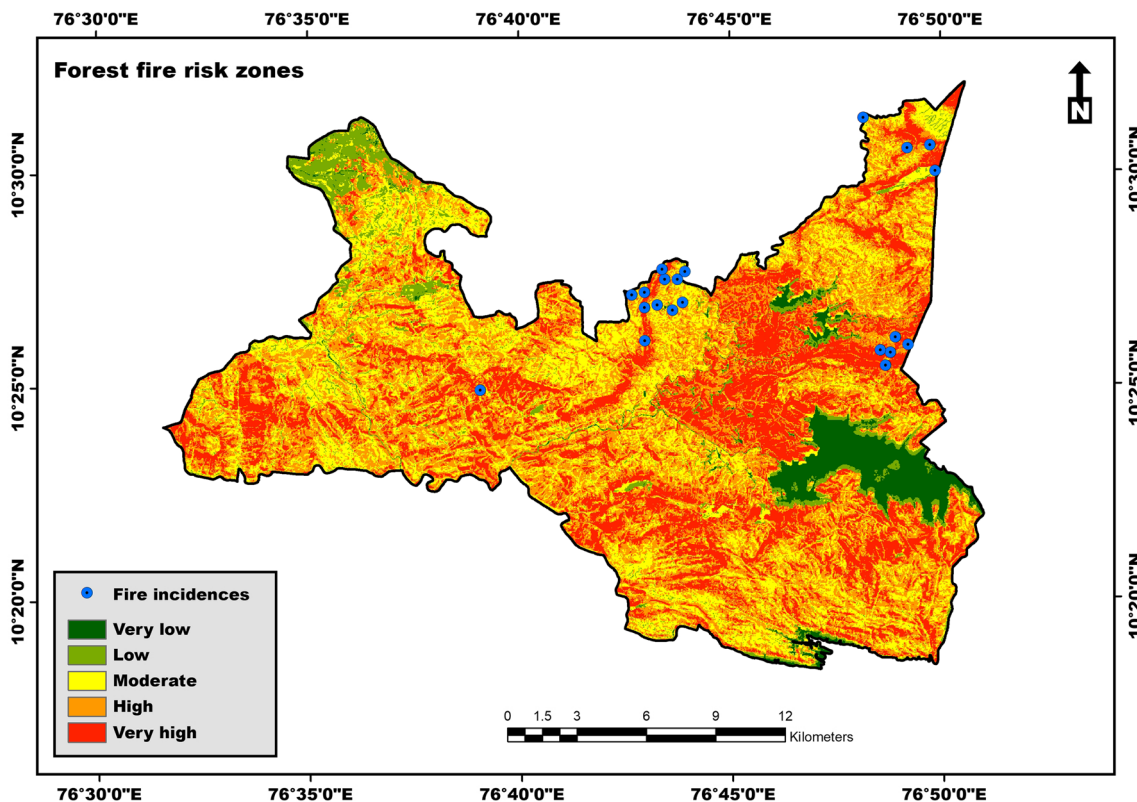


Fig. 11 Forest fire risk zones

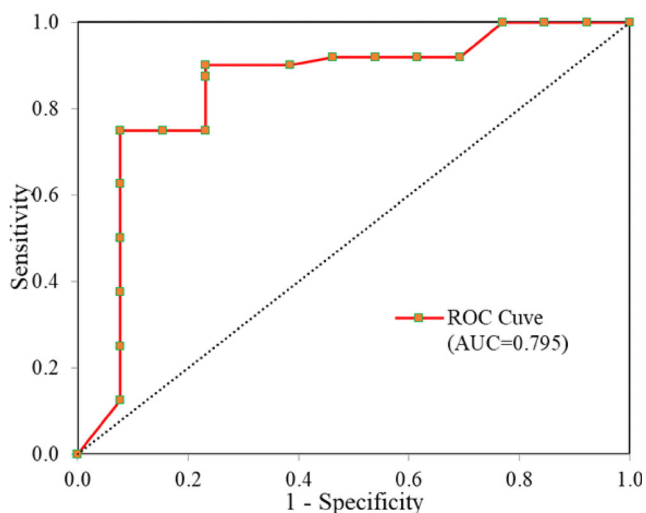


Fig. 12 ROC curve

fires. In close proximity to the camp sheds, a large number of fire incidences (14) occurred. This reaffirms the requirement of fire watchtowers and efficient monitoring in this area. In this study, the ROC curve with an AUC value of 0.795 shows that the prepared risk zone map is acceptable (Fig. 12).

Conclusions

The present study demarcated the forest fire risk zones in PKMTR using geospatial tools and assessed the influence of various factors on fire initiation. This study classified PKMTR into the following five risk zones: very low, low, moderate, high, and very high. The high-risk and very high-risk zones together constitute 61.92% of the study area. It was found that the factors such as topographic wetness index, roads, and settlements demonstrate a strong correlation with forest fire occurrences. This confirms the anthropogenic origin of fires. From the study, it was observed that 71% of fire incidences spatially fall over the high-risk and very high-risk zones. The ROC curve analysis with an AUC value of 0.795 proves the acceptability of the result. This study suggests the requirement of fire watchtowers and effective fire monitoring in areas with more fire events. The risk zone map will help land use planners and decision-makers to establish fire protection strategies for identifying appropriate locations for fire watchtowers, fire lines, sensors installation, etc., in order to minimize potential impacts of fire.

Declarations

Ethics Approval and Consent to Participate This article does not contain any studies with human participants or animals performed by any of the authors. Informed consent is not applicable.

Conflict of Interest The authors declare no competing interests.

References

- Abdi O, Kamkar B, Shirvani Z, da Silva JAT, Buchroithner MF (2018) Spatial-statistical analysis of factors determining forest fires: a case study from Golestan, Northeast Iran. *Geom. Nat Hazards Risk* 9(1): 267–280. <https://doi.org/10.1080/19475705.2016.1206629>
- Ajin RS, Jacob MK, Menon ARR, Vinod PG (2014) Forest fire risk analysis using geo-information technology: a study of Peppara Wildlife Sanctuary, Thiruvananthapuram, Kerala, India. In: Pradeep Kumar AP, Behr FJ, Illiyas FT, Shaji E (eds) *Proceedings of the 2nd Disaster Risk Vulnerability Conference 2014 (DRVC-2014)*. Thiruvananthapuram, India, pp 160–165
- Ajin RS, Loghin AM, Jacob MK, Vinod PG, Krishnamurthy RR (2016a) The risk assessment of potential forest fire in Idukki Wildlife Sanctuary using RS and GIS techniques. *Int J Adv Earth Sci Eng* 5(1):308–318
- Ajin RS, Loghin AM, Vinod PG, Jacob MK (2016b) Forest fire risk zone mapping in Chinnar Wildlife Sanctuary, Kerala, India: a study using geospatial tools. *J Global Res* 3:16–26
- Ajin RS, Loghin AM, Vinod PG, Jacob MK (2016c) Forest fire risk zone mapping using RS and GIS techniques: a study in Achankovil forest division, Kerala, India. *J Earth Environ Health Sci* 2(3):109–115. <https://doi.org/10.4103/2423-7752.199288>
- Ajin RS, Loghin AM, Vinod PG, Jacob MK (2017a) Mapping of forest fire risk zones in Peechi-Vazhani Wildlife Sanctuary, Thrissur, Kerala, India: a study using geospatial techniques. *J Wetlands Biodiver* 7:7–16
- Ajin RS, Loghin AM, Vinod PG, Jacob MK (2017b) The risk analysis of potential forest fires in a wildlife sanctuary in the Western Ghats (Southwest Indian Peninsula) using geospatial techniques. *Int J Health Syst Disaster Manag* 5(1):18–23. https://doi.org/10.4103/ijhsdm.ijhsdm_26_16
- Ajin RS, Loghin AM, Vinod PG, Menon ARR, Jacob MK (2018) Forest fire risk assessment using geospatial techniques: a study in Mannarkkad forest division of Palakkad District, Kerala, India. *ECOTERRA - J Environ Res Protect* 15(1):1–9
- Ambadan JT, Oja M, Gedalof Z, Berg AA (2020) Satellite-observed soil moisture as an indicator of wildfire risk. *Remote Sens* 12(10). <https://doi.org/10.3390/rs12101543>
- Arca D, Hacısalihoğlu M, Kutoğlu ŞH (2020) Producing forest fire susceptibility map via multi-criteria decision analysis and frequency ratio methods. *Nat Hazards* 104:73–89. <https://doi.org/10.1007/s11069-020-04158-7>
- Arpaci A, Malowerschnig B, Sass O, Vacik H (2014) Using multi variate data mining techniques for estimating fire susceptibility of Tyrolean forests. *Appl Geogr* 53:258–270. <https://doi.org/10.1016/j.apgeog.2014.05.015>
- Beven KJ, Kirkby MJ (1979) A physically based, variable contributing area model of basin hydrology. *Hydrol Sci J* 24(1):43–69. <https://doi.org/10.1080/02626667909491834>
- Bui DT, Bui QT, Nguyen QP, Pradhan B, Nampak H, Trinh PT (2017) A hybrid artificial intelligence approach using GIS-based neural-fuzzy inference system and particle swarm optimization for forest fire susceptibility modeling at a tropical area. *Agric For Meteorol* 233: 32–44. <https://doi.org/10.1016/j.agrformet.2016.11.002>
- Busico G, Giuditta E, Kazakis N, Colombani N (2019) A hybrid GIS and AHP approach for modelling actual and future forest fire risk under climate change accounting water resources attenuation role. *Sustainability* 11. <https://doi.org/10.3390/su11247166>
- Certini G (2005) Effects of fire on properties of forest soils: a review. *Oecologia* 143:1–10. <https://doi.org/10.1007/s00442-004-1788-8>
- Chen Z (2006) Effects of fire on major forest ecosystem processes: an overview. *Ying Yong Sheng Tai Xue Bao (J Appl Ecol)* 17(9): 1726–1732

- Deng O, Su G, Huang Q, Li Y (2013) Forest fire risk mapping based on spatial logistic model of Northeastern China forest zone. In: Bian F, Xie Y, Cui X, Zeng Y (eds) *Geo-Informatics in Resource Management and Sustainable Ecosystem (GRMSE 2013)*, Communications in Computer and Information Science, vol 399. Springer, Berlin, pp 181–192. https://doi.org/10.1007/978-3-642-41908-9_18
- Dong X, Li-min D, Guo-fan S, Lei T, Hui W (2005) Forest fire risk zone mapping from satellite images and GIS for Baihe Forestry Bureau, Jilin, China. *J For Res* 16:169–174. <https://doi.org/10.1007/BF02856809>
- Dimuccio LA, Ferreira R, Cunha L, de Almeida AC (2011) Regional forest-fire susceptibility analysis in central Portugal using a probabilistic ratings procedure and artificial neural network weights assignment. *Int J Wildland Fire* 20(6):776–791. <https://doi.org/10.1071/WF09083>
- Eskandari S (2017) A new approach for forest fire risk modeling using fuzzy AHP and GIS in Hyrcanian forests of Iran. *Arab J Geosci* 10. <https://doi.org/10.1007/s12517-017-2976-2>
- Eskandari S, Miesel JR (2017) Comparison of the fuzzy AHP method, the spatial correlation method, and the Dong model to predict the fire high-risk areas in Hyrcanian forests of Iran. *Geom, Nat Hazards Risk* 8(2):933–949. <https://doi.org/10.1080/19475705.2017.1289249>
- Estes BL, Knapp EE, Skinner CN, Miller JD, Preisler HK (2017) Factors influencing fire severity under moderate burning conditions in the Klamath Mountains, Northern California, USA. *Ecosphere* 8(5). <https://doi.org/10.1002/ecs2.1794>
- Finlay SE, Moffat A, Gazzard R, Baker D, Murray V (2012) Health impacts of wildfires. *PLOS Curr Disast*. <https://doi.org/10.1371/4f959951cce2c>
- Flach PA (2011) ROC Analysis. In: Sammut C, Webb GI (eds) *Encyclopedia of machine learning*. Springer, Boston. https://doi.org/10.1007/978-0-387-30164-8_733
- Franzen MD (2011) Receiver-operating characteristics. In: Kreutzer JS, DeLuca J, Caplan B (eds) *Encyclopedia of clinical neuropsychology*. Springer, New York, NY. https://doi.org/10.1007/978-0-387-79948-3_1240
- Gheshlaghi HA (2019) Using GIS to develop a model for forest fire risk mapping. *J Indian Soc Remote Sens* 47(7):1173–1185. <https://doi.org/10.1007/s12524-019-00981-z>
- Gheshlaghi HA, Feizizadeh B, Blaschke T (2020) GIS-based forest fire risk mapping using the analytical network process and fuzzy logic. *J Environ Plan Manag* 63(3):481–499. <https://doi.org/10.1080/09640568.2019.1594726>
- Güngöroğlu C (2017) Determination of forest fire risk with fuzzy analytic hierarchy process and its mapping with the application of GIS: the case of Turkey/Çakırlar. *Human Ecologic Risk Assess: Int J* 23(2): 388–406. <https://doi.org/10.1080/10807039.2016.1255136>
- Hanley JA, McNeil BJ (1982) The meaning and use of the area under a receiver operating characteristic (ROC) curve. *Radiology* 143(1): 29–36. <https://doi.org/10.1148/radiology.143.1.7063747>
- Hong H, Tsangaratos P, Ilia I, Liu J, Zhu AX, Xu C (2018) Applying genetic algorithms to set the optimal combination of forest fire related variables and model forest fire susceptibility based on data mining models. The case of Dayu County, China. *Sci Total Environ* 630:1044–1056. <https://doi.org/10.1016/j.scitotenv.2018.02.278>
- Hosmer DW, Lemeshow S (2000) *Applied logistic regression*, 2nd edn. John Wiley & Sons, Inc., United States of America, p 392
- Jaiswal RK, Mukherjee S, Raju KD, Saxena R (2002) Forest fire risk zone mapping from satellite imagery and GIS. *Int J Appl Earth Obs Geoinf* 4(1):1–10. [https://doi.org/10.1016/S0303-2434\(02\)00006-5](https://doi.org/10.1016/S0303-2434(02)00006-5)
- Jobin KM, Nameer PO (2012) Diversity of rhacophorids (Amphibia: Anura) in Parambikulam Tiger Reserve, Western Ghats, Kerala, India. *J Threat Taxa* 4(13):3205–3214. <https://doi.org/10.11609/JoTT.o3081.3205-14>
- Kaur H, Sood SK (2019) Adaptive neuro fuzzy inference system (ANFIS) based wildfire risk assessment. *J Exper Theoret Artif Intellig* 31(4):599–619. <https://doi.org/10.1080/0952813X.2019.1591523>
- Kayet N, Chakrabarty A, Pathak K, Sahoo S, Dutta T, Hatai BK (2020) Comparative analysis of multi-criteria probabilistic FR and AHP models for forest fire risk (FFR) mapping in Melghat Tiger Reserve (MTR) forest. *J For Res* 31:565–579. <https://doi.org/10.1007/s11676-018-0826-z>
- Kil SH, Lee DK, Kim JH, Li MH, Newman G (2016) Utilizing the analytic hierarchy process to establish weighted values for evaluating the stability of slope revegetation based on hydroseeding applications in South Korea. *Sustainability* 8(1). <https://doi.org/10.3390/su8010058>
- Krueger ES, Ochsner TE, Engle DM, Carlson JD, Twidwell D, Fuhlendorf SD (2015) Soil moisture affects growing-season wildfire size in the Southern Great Plains. *Soil Sci Soc Am J* 79(6):1567–1576. <https://doi.org/10.2136/sssaj2015.01.0041>
- Leuenberger M, Parente J, Tonini M, Pereira MG, Kanevski M (2018) Wildfire susceptibility mapping: deterministic vs. stochastic approaches. *Environ Model Softw* 101:194–203. <https://doi.org/10.1016/j.envsoft.2017.12.019>
- Manna I, Bandyopadhyay M (2019) Chapter 16 - Physicochemical perturbation of plants on exposure to metal oxide nanoparticle. In: Tripathi DK, Ahmad P, Sharma S, Chauhan DK, Dubey NK (eds) *Nanomaterials in plants, algae and microorganisms: concepts and controversies*, vol 2. Academic Press, pp 323–352. <https://doi.org/10.1016/B978-0-12-811488-9.00016-0>
- Martin D, Tomida M, Meacham B (2016) Environmental impact of fire. *Fire Sci Rev* 5. <https://doi.org/10.1186/s40038-016-0014-1>
- Melo F (2013) Area under the ROC curve. In: Dubitzky W, Wolkenhauer O, Cho KH, Yokota H (eds) *Encyclopedia of systems biology*. Springer, New York. https://doi.org/10.1007/978-1-4419-9863-7_209
- Mohammadi F, Bavaghar MP, Shabani N (2014) Forest fire risk zone modeling using logistic regression and GIS: an Iranian case study. *Small-scale Forestry* 13:117–125. <https://doi.org/10.1007/s11842-013-9244-4>
- Nadporozhskaya MA, Chertov OG, Bykhovets SS, Shaw CH, Maksimova EY, Abakumov EV (2018) Recurring surface fires cause soil degradation of forest land: a simulation experiment with the EFIMOD model. *Land Degrad Dev* 29(7):2222–2232. <https://doi.org/10.1002/ldr.3021>
- Nameer PO, Molur S, Walker S (2001) Mammals of Western Ghats: a simplistic overview. *Zoos' Print J* 16(11):629–639
- Nuthammachot N, Stratoulas D (2019) A GIS- and AHP-based approach to map fire risk: a case study of Kuan Kreng peat swamp forest, Thailand. *Geocarto Int* 36:212–225. <https://doi.org/10.1080/10106049.2019.1611946>
- Novo A, Fariñas-Álvarez N, Martínez-Sánchez J, González-Jorge H, Fernández-Alonso JM, Lorenzo H (2020) Mapping forest fire risk - a case study in Galicia (Spain). *Remote Sens* 12(22). <https://doi.org/10.3390/rs12223705>
- Pan J, Wang W, Li J (2016) Building probabilistic models of fire occurrence and fire risk zoning using logistic regression in Shanxi Province, China. *Nat Hazards* 81:1879–1899. <https://doi.org/10.1007/s11069-016-2160-0>
- Pastro LA, Dickman CR, Letnic M (2011) Burning for biodiversity or burning biodiversity? Prescribed burn vs. wildfire impacts on plants, lizards, and mammals. *Ecol Appl* 21(8):3238–3253. <https://doi.org/10.1890/10-2351.1>
- Pourtaghi ZS, Pourghasemi HR, Aretano R, Semeraro T (2016) Investigation of general indicators influencing on forest fire and its

- susceptibility modeling using different data mining techniques. *Ecol Indic* 64:72–84. <https://doi.org/10.1016/j.ecolind.2015.12.030>
- Pradhan B, Suliman MDHB, Awang MAB (2007) Forest fire susceptibility and risk mapping using remote sensing and geographical information systems (GIS). *Disaster Prev Manag* 16(3):344–352. <https://doi.org/10.1108/09653560710758297>
- Ricotta C, Bajocco S, Guglietta D, Conedera M (2018) Assessing the influence of roads on fire ignition: does land cover matter? *Fire* 1(2). <https://doi.org/10.3390/fire1020024>
- Saaty TL (1980) *The analytic hierarchy process: planning, priority setting, resource allocation (decision making series)*. McGraw Hill, New York
- Sannigrahi S, Pilla F, Basu B, Basu AS, Sarkar K, Chakraborti S, Joshi PK, Zhang Q, Wang Y, Bhatt S, Bhatt A, Jha S, Keesstra S, Roy PS (2020) Examining the effects of forest fire on terrestrial carbon emission and ecosystem production in India using remote sensing approaches. *Sci Total Environ* 725:138331. <https://doi.org/10.1016/j.scitotenv.2020.138331>
- Santín C, Doerr SH (2016) Fire effects on soils: the human dimension. *Philosophical transactions of the Royal Society of London. Ser B, Biol Sci* 371(1696). <https://doi.org/10.1098/rstb.2015.0171>
- Satir O, Berberoglu S, Donmez C (2016) Mapping regional forest fire probability using artificial neural network model in a Mediterranean forest ecosystem. *Geom, Nat Hazards Risk* 7(5):1645–1658. <https://doi.org/10.1080/19475705.2015.1084541>
- Setiawan I, Mahmud AR, Mansor S, Shariff ARM, Nuruddin AA (2004) GIS-grid-based and multi-criteria analysis for identifying and mapping peat swamp forest fire hazard in Pahang, Malaysia. *Disaster Prev Manag* 13(5):379–386. <https://doi.org/10.1108/09653560410568507>
- Soman D, Anitha V (2020) Community dependence on the natural resources of Parambikulam Tiger Reserve, Kerala, India. *Trees, Forests People* 2:100014. <https://doi.org/10.1016/j.tfp.2020.100014>
- Soto MEC (2012) The identification and assessment of areas at risk of forest fire using fuzzy methodology. *Appl Geogr* 35(1-2):199–207. <https://doi.org/10.1016/j.apgeog.2012.07.001>
- Sreehari R, Nameer PO (2016) Small carnivores of Parambikulam Tiger Reserve, Southern Western Ghats, India. *J Threat Taxa* 8(11):9306–9315. <https://doi.org/10.11609/jott.2311.8.11.9306-9315>
- Tedim F, Garcin M, Vinchon C, Carvalho S, Desramaut N, Rohmer J (2014) Chapter 7 - Comprehensive vulnerability assessment of forest fires and coastal erosion: evidences from case-study analysis in Portugal. In: Birkmann J, Kienberger S, Alexander DE (eds) *Assessment of vulnerability to natural hazards*. Elsevier, Netherlands, pp 149–177. <https://doi.org/10.1016/B978-0-12-410528-7.00007-2>
- Tiwari A, Shoab M, Dixit A (2020) GIS-based forest fire susceptibility modeling in Pauri Garhwal, India: a comparative assessment of frequency ratio, analytic hierarchy process and fuzzy modeling techniques. *Nat Hazards* 105:1189–1230. <https://doi.org/10.1007/s11069-020-04351-8>
- Veena HS, Ajin RS, Loghin AM, Sipai R, Adarsh P, Viswam A, Vinod PG, Jacob MK, Jayaprakash M (2017) Wildfire risk zonation in a tropical forest division in Kerala, India: a study using geospatial techniques. *Int J Conserv Sci* 8(3):475–484
- Vinod PG, Ajin RS, Jacob MK (2016) RS and GIS based spatial mapping of forest fire risk zones in Wayanad Wildlife Sanctuary, North Kerala, India. *Int J Earth Sci Eng* 9(2):498–502
- Ye J, Wu M, Deng Z, Xu S, Zhou R, Clarke KC (2017) Modeling the spatial patterns of human wildfire ignition in Yunnan province, China. *Appl Geogr* 89:150–162. <https://doi.org/10.1016/j.apgeog.2017.09.012>
- Yin HW, Kong FH, Li XZ (2004) RS and GIS-based forest fire risk zone mapping in da Hinggan mountains. *Chin Geogr Sci* 14:251–257. <https://doi.org/10.1007/s11769-003-0055-y>
- Yong B, Ren LL, Hong Y, Gourley JJ, Chen X, Zhang YJ, Yang XL, Zhang ZX, Wang WG (2012) A novel multiple flow direction algorithm for computing the topographic wetness index. *Hydrol Res* 43(1-2):135–145. <https://doi.org/10.2166/nh.2011.115>
- Gigović L, Pourghasemi HR, Drobnjak S, Bai S (2019) Testing a new ensemble model based on SVM and random forest in forest fire susceptibility assessment and its mapping in Serbia's Tara National Park. *Forests* 10(5). <https://doi.org/10.3390/f10050408>

Publisher's Note Springer Nature remains neutral with regard to jurisdictional claims in published maps and institutional affiliations.